

THEORY AND TEST OF COMMERCIALY AVAILABLE WOLTER
PHASEPLATE FOR USE IN SCHLIEREN OPTICAL SYSTEMS
EMPLOYED IN ULTRACENTRIFUGATION AND ELECTROPHORESIS*

by

RODES TRAUTMAN AND VICTOR W. BURNS

*Radiation Laboratory, Donner Laboratory of Medical Physics, University of California,
Berkeley, California (U.S.A.)*

In 1950 WOLTER¹ described a new type of schlieren diaphragm² which utilized Fresnel diffraction effects to yield on the photographic plate or ground glass of the schlieren camera a pattern which has an intensity null at the true boundary position. In contrast to diaphragms with mechanical straight edges from opaque elements such as a blade, bar, wire or slit, WOLTER's completely transparent "phaseplate" employs an optical edge. The optical edge is the discontinuity at the edge of a uniform transparent coating over half of a supporting transparent glass plate. The coating is thus similar in size and position to the half plane or blade, except that it is transparent and of such a thickness that transmitted rays will be one half a wavelength out of phase with adjacent rays not passing through the coating. The phaseplate edge can give a shadow on the ground glass only if the light source image does not focus on it (*i.e.* does not focus in the plane of the schlieren diaphragm). Thus straight baselines in principle give no registration but peaks do, since boundary regions in a parallel wall cell defocus the light source image as well as deflect it^{3,4}. Each level in a boundary region can thus be represented by a prism accounting for the deflection and a lens accounting for the defocusing (schematically shown in Fig. 6). It is this defocused light source image illuminating the mechanical schlieren diaphragm which casts the familiar Fresnel type diffraction pattern on the photographic plate⁵. Various ways of obtaining the baseline and regions where there is no lens action (*e.g.* top of peak) are available when using a phaseplate: a. the edge of the phaseplate can be centered in a mechanical slit^{6,7}. The baseline is obtained by bisecting the slit pattern which is well defined in those regions in which the phaseplate pattern is missing. b. A very narrow wire (about $1/4$ – $1/3$ diameter of a wire suitable for a diaphragm) gives the baseline regions but no peaks. Hence the superposition of the wire accurately along the optical edge of the phaseplate gives both baselines and pattern of essentially the same width for all deflections. An example of this appears later (Fig. 2a). c. A third way is to defocus the light source, but this gives tilted baselines. d. A fourth way is to avoid overexposure and use the very faint, extremely sharp line which does appear due probably to imperfections in the phaseplate.

* This work was supported (in part) by the Atomic Energy Commission and by a grant from the Life Insurance Medical Research Fund.

Several methods of making a phaseplate were suggested by WOLTER¹. These were all tried unsuccessfully in this laboratory. It was only when the American Optical Company, Instrument Division, Buffalo, N.Y., experts in phase coatings, was contacted that a usable phaseplate was obtained. The coating is MgF_2 evaporated onto the supporting plate, and is sufficiently durable that it can be cleaned with methanol and lens paper, and no cover glass is necessary. The cost of the coating is nominal; the price of the complete phaseplate being determined mainly by the choice of the supporting glass as to a. optical quality b. size and c. shape, including notches or holes for mounting purposes.

The purpose of this paper is to describe test experiments with the phaseplates and present in greater detail the theory of its operation in a schlieren optical system.

EXPERIMENTAL

The tests of the phaseplates supplied by the American Optical Company for the mercury green line were made on both a Klett electrophoresis apparatus and Spinco Model E ultracentrifuge. The plates were supplied round and notched so that they could be cemented to a brass ring which was attached to the diaphragm mount (see Fig. 1). The coating has a slight greenish tinge to it which has a negligible effect on its transparency. For the comparison pictures the brass ring had simultaneously a wire (0.010" diameter) and/or a standard Spinco bar (1.5 mm). The phaseplates were made from ordinary plate glass. Ideally, one would prefer an optical flat, but only a small region (approx. 1 mm) on either side of the edge is used, and repolished plate glass was found satisfactory. An unpolished plate glass with an observable "orange peel" surface gave good patterns except for the mottled background due directly to this "orange peel" surface (see Fig. 2a). This figure also shows application of a wire 0.003" dia. along the phaseplate edge to register baseline regions. It is essential that the edge be sharp, for if it is not, it acts like a cylinder lens and discriminates between the rays of the same deflection coming from the two sides of the boundary region. This causes a distortion of the pattern and is easily detected on a symmetrical gradient because the diffraction fringes inside the peak do not cross at the center (see Fig. 2b).

Fig. 3a shows the appearance of a boundary in the ultracentrifuge with a wire (top), phaseplate (center) and a bar (bottom). The three diaphragms were parallel and used simultaneously. The synthetic boundary cell⁸ was used to get the boundary in the center of the cell. The double meniscus is due to a layer of mineral oil on the protein solution. Notice that the baseline is almost invisible with the phaseplate. Observe also that the diffraction fringes have greater contrast than the ones of the wire or bar (a point to be discussed theoretically later) and have essentially the same horizontal spacing for the three diaphragms at any chosen height above the baseline. Fig. 3b shows the same test on the Klett electrophoresis apparatus. Two exposures are shown. The phaseplate pattern remains sharp over a wide range of exposure, losing the baseline on overexposure. This is in contrast to the wire pattern which loses the peak relative to the baseline. On overexposure the bar pattern reveals diffraction fringes inside, as pointed out previously by KEGELES⁹. It has been the experience in this laboratory that the obscure condition mentioned by Wolter on the size of the light source slit is inapplicable, and all the pictures of this paper have been taken with conventional slit openings and exposure times. It has been observed, also (but not illustrated here by a photograph) that increasing the light source slit width to as much as 0.5 mm is equivalent to increasing the exposure as far as sharpness of detail is concerned. Hence stringent conditions on light source slit width are in practice not necessary. Areas were measured under the curves of Fig. 3a and 3b with the result

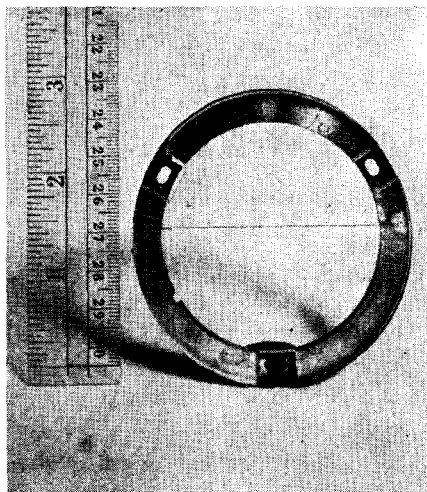


Fig. 1. Phaseplate mounted on brass ring. Lower half is coated to a line 2 mm below the wire shown.

that the average of the bar patterns agreed with the wire and phaseplate within the plate reading error of $\pm 1\%$.

Fig. 3c shows the boundary of Fig. 3a taken at very high magnification (small angle of the phaseplate as schlieren diaphragm). The wire or bar patterns at this magnification would be unusable. Thus the phaseplate retains its very narrow registration of the boundary (geometrical shadow) over the entire range of diaphragm angles. The phaseplate also retains its excellent registration for both steep and shallow gradient curves. This is in direct contrast to the wire pattern which becomes poorer as the curve becomes steeper. This is shown in Fig. 4b which is the sixth frame of a standard lipoprotein¹⁰ run, using a single cell but the wire (upper pattern) and the phaseplate (lower pattern) simultaneously for comparison purposes. Compare the appearance of the pattern

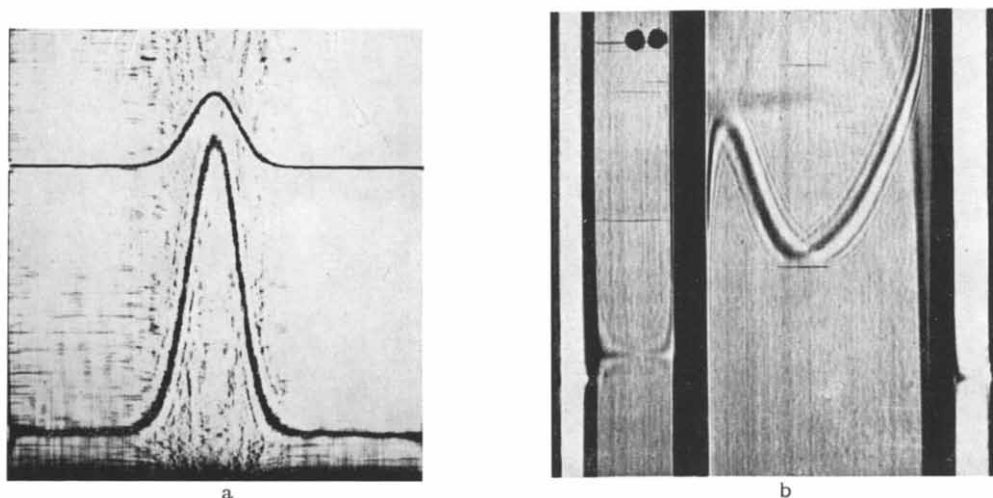


Fig. 2. Special imperfect phaseplates. a. Unpolished plate glass; b. Rounded edge of phaseplate coating. In spite of the mottled background, the phaseplate in a. gives legible patterns. The baseline regions have been made visible by attaching a fine wire (0.003" dia.) along the phaseplate edge.

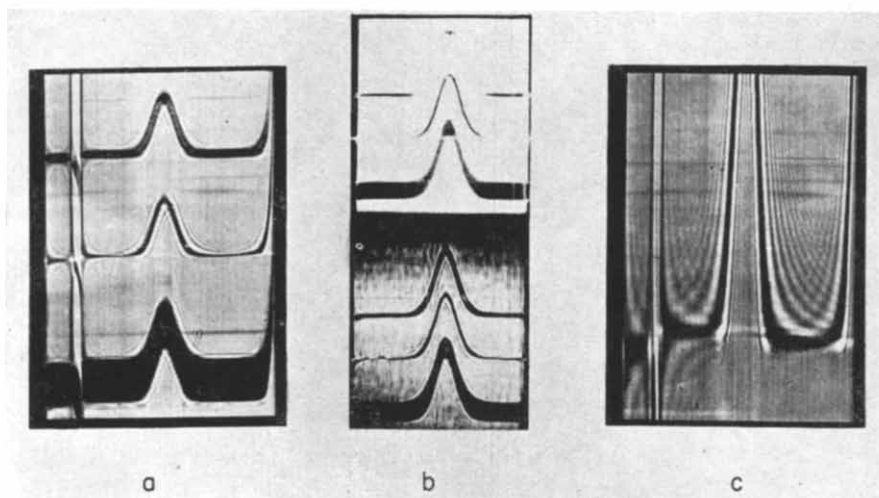


Fig. 3. Comparison of bar, wire and phaseplate as schlieren diaphragm simultaneously. a and b. Upper pattern: 0.010" wire; Middle pattern: Phaseplate; Lower pattern: 1.5 mm bar. a. Ultra-centrifuge. Synthetic boundary cell. Mineral oil on top of protein solution. b. Electrophoresis. Two exposures shown. Above: Overexposure; Below: Normal exposure. c. High magnification (15° diaphragm angle) of phaseplate pattern of a.

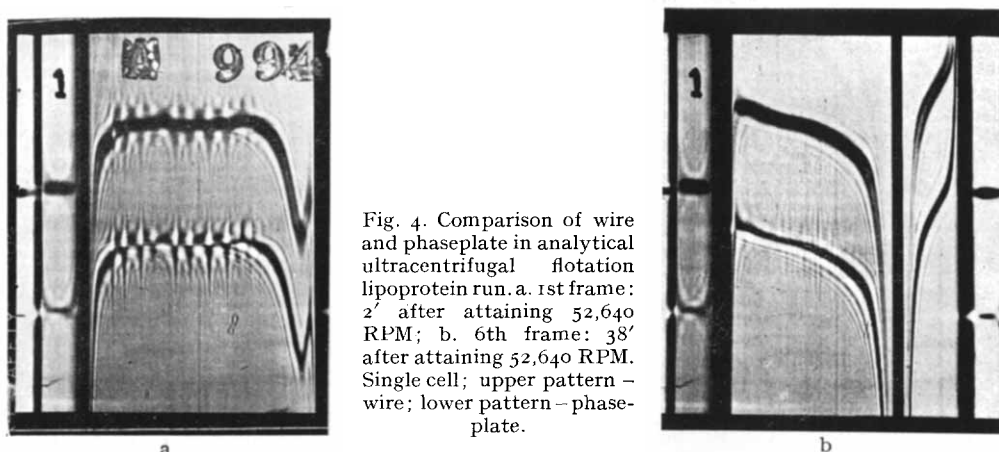


Fig. 4. Comparison of wire and phaseplate in analytical ultracentrifugal flotation lipoprotein run. a. 1st frame; 2' after attaining 52,640 RPM; b. 6th frame: 38' after attaining 52,640 RPM. Single cell; upper pattern - wire; lower pattern - phaseplate.

in the neighbourhood of the vertical bar for the wire and the phaseplate. Disturbances in the cell sometimes encountered in sedimenting as well as floating runs are usually much more vividly portrayed by the phaseplate than the wire or bar. An example of this is shown in Fig. 4a, where the upper pattern is the wire and lower pattern is the phaseplate.

There is an outstanding anomaly of all schlieren diaphragms in which the inside pattern appears with sharper "corners" than does the outside pattern at the tails of a bell-shaped peak. This is evident on the bar pattern of Fig. 3a and 3b and can be seen also on blade (knife edge) patterns if one reverses the blade so as to compare black on white and white on black patterns. The pattern in which the knife edge cuts out the undeflected light source image as well as deflected rays (opaque upper half-plane in electrophoresis, for example) will have sharper corners than the usual pattern in which the inside of the bell-shaped peak is a shadow region. With the phaseplate, since outside and inside patterns are merged to a single null-point registration, the nature of this anomaly becomes clear. It is due to the closer spacing of the diffraction fringes inside the pattern as compared to outside. This is seen on all the pictures but most vividly on Fig. 3c. The steeper the gradient, the greater is this effect. Since the theory of the diffraction patterns, to be presented below, indicates only symmetrical diffraction patterns, this anomaly of the schlieren optical system poses a serious question as to whether in these regions there is accurate registration of the boundary. Thus, the averaging of inside and outside patterns with the bar, for example, takes care of size changes due to exposure variations but does not take care of this difference in shape of inside and outside pattern. An attractive hypothesis for the explanation of the closer spacing of fringes inside the pattern is that the light rays from the two sides of the boundary with the same deflection are somehow interacting to yield the diffraction pattern inside, but effectively are independent for the diffraction pattern outside. In Fig. 6, to be explained when the theory is considered, the light source images at G and H from the two sides of the boundary would be considered as simultaneously casting an interfering Fresnel type diffraction pattern. As a test of this hypothesis a boundary was formed in the macro electrophoresis cell (7.5 mm channel width) so that the boundary region would be wide enough, left and right, to enable masking out, at the cell, light from one side of the boundary, and then the other side, leaving a vertical strip down the center of the cell which was not masked at all. If the hypothesis were correct, then the closer spacing in the center of the channel, inside the boundary,

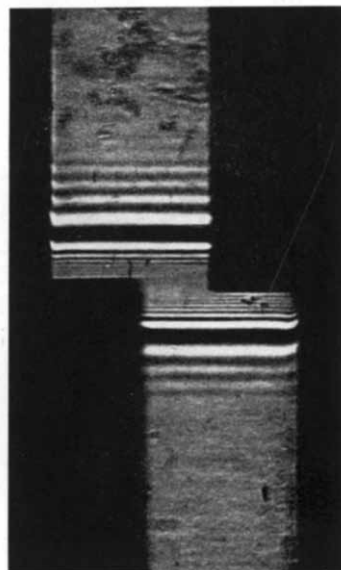


Fig. 5. Anomalous diffraction effect. Selective masking of certain boundary regions showing independence of light rays of the same deflection in determining the Fresnel diffraction pattern which has closer spacing inside the boundary than outside. Horizontal phaseplate in scanning schlieren camera. Solvent (upper) buffer, solution (lower), 0.3% protein. Left, masking out solution side of boundary max. gradient, right, masking out of solvent side of boundary max. gradient.

would become greater and equal to that outside the boundary left and right of the center where the masks were placed. Fig. 5 shows the resulting photograph for one setting of the phaseplate in the electrophoresis apparatus. No cylindrical lens is used and the phaseplate is horizontal, representing one position in a scanning type pattern. It can be seen that the spacing inside the two sides of the boundary is closer than outside (which incidentally shows that the anomaly is not due to the cylindrical lens and/or the diaphragm being diagonal). But the spacing is *not* altered by the masks. Therefore the hypothesis is false that the spacing inside is due to the interaction of light from the two sides of the boundary that have the same deflection. Hence, this phenomenon remains unexplained, and perhaps must wait explanation until the schlieren optical system is handled completely by physical optics from the light source to the photographic plate, rather than mixing geometrical and physical optics as indicated in the theory below.

Theory of the spacing of the fringes "outside" the geometrical shadow

There are two methods in the literature for deriving the expressions for the Fresnel fringes in the schlieren optical system. Both consider the schlieren camera without the cylindrical lens. However, the schlieren optical set-up without the cylindrical lens is still quite complex and in the usual arrangement the camera objective is between the diffracting edge (schlieren diaphragm) and the photographic plate. To avoid this complication DISTÈCHE¹¹ refers all optical components to the neighbourhood of the cell by geometrical optics, then treats the interaction of these elements by physical optics to get the intensity distribution in the plane, in this neighbourhood, which by geometrical optics is imaged on the photographic plate. The details of the derivation are obscure, but the resulting fringe spacings are those of Fresnel diffraction from a knife edge. The absolute magnitude of the spacings in terms of the refractive index distribution and optical constants is $\sqrt{2}$ times as large as the spacing predicted from WOLTER's theory (if it is applied to the same diffracting element, a knife edge).

WOLTER¹, on the other hand, chooses an equivalent optical system which has no lenses between the schlieren diaphragm and the photographic plate. This is shown in Fig. 6. (Various equivalent optical systems are given by SVENSSON⁴.) Geometrical optics are used to find the location of the light source after rays pass through the schlieren lens, the gradient lens, and the second schlieren lens acting also as a camera objective. This (defocused) light source image is considered the source, the schlieren diaphragm the diffracting element, and the photographic plate the screen in the conventional

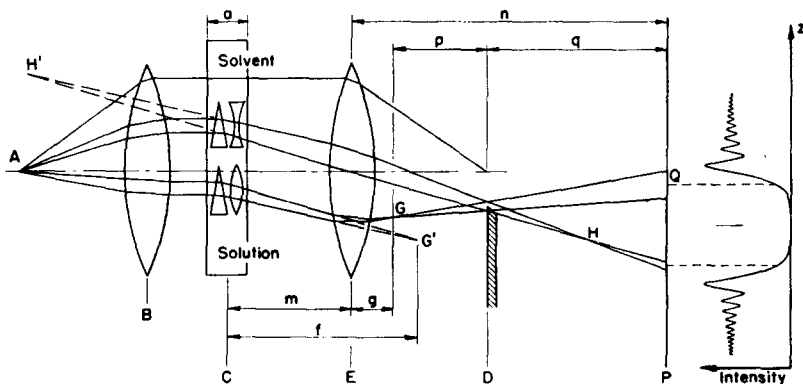


Fig. 6. Schematic equivalent schlieren optical system. A. Light source; B. (First) schlieren lens; C. Cell; D. Schlieren diaphragm; E. (Second) schlieren lens and camera objective; G. Light source image for rays passing through solution side of max. refractive index gradient; H. Light source image for rays passing through solvent side of max. ref. index gradient; P. Photographic plate or ground glass.

Fresnel type diffraction problem. The method is only outlined by WOLTER. Since it gives an insight into the schlieren optical system and allows derivation of fringe spacings (other than the anomaly mentioned earlier) for any type of diaphragm one may choose to use, the details are considered here. Because of the equivalence of the various schlieren optical systems the conclusions for the one of Fig. 6 are assumed valid in any system, including the diagonal slit, cylindrical lens set-up.

First consider the lens action of the gradient. This has been described^{3,4} but a simple derivation will be given here. In Fig. 7 the cell is shown illuminated by two parallel rays. By definition, the focal length of the equivalent lens is the distance to the point of focus when illuminated by parallel light. From the drawing, $-d\delta = dz/f$ where according to convention the upward direction of z is positive and focal length f is positive if the focal point is to the right of the cell. But the deflection of light passing through an index of refraction gradient is $\delta = a dn/dz$ where a is the cell path length and n is the index of refraction of the solution in the cell at the location of the ray considered. Thus:

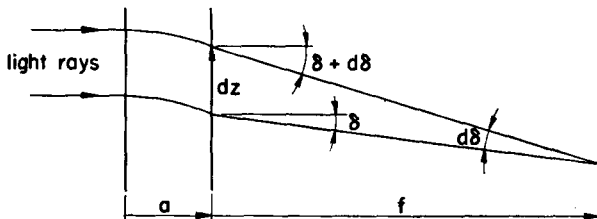


Fig. 7. Lens action of a refractive index gradient.

$$f = -\frac{dz}{d\delta} = -\frac{1}{a \frac{d^2n}{dz^2}} = -\frac{1}{a n''} \quad (1)$$

The lens E of focal length b focuses the cell C on the plate P according to the lens formula

$$\frac{1}{m} + \frac{1}{n} = \frac{1}{b} \quad (2)$$

Its magnification M is expressible from (2) as

$$M = \frac{n}{m} = \frac{n-b}{b} \quad (3)$$

Rays through two portions of the boundary region are drawn in Fig. 6. The two regions are on either side of the maximum refractive index gradient and have the same deflection. The effect of the gradient is schematically shown by the insert figures of a prism and a lens. The solvent side of the maximum gradient is concave, hence is a diverging lens, whereas the solution side is convex (on a c vs z plot) and is a converging lens. Just the converging side is considered. It focuses the light source at G' which is now imaged by the lens E to the point G by the lens formula

$$\frac{1}{m-f} + \frac{1}{g} = \frac{1}{b} \quad (4)$$

Solving this for $b - g$, the distance p of the source from the diffracting element, gives:

$$p \equiv b - g = -\frac{b^2}{m - b - f} \quad (5)$$

The distance of the screen from the plate is

$$q \equiv n - b \quad (6)$$

Now in the Fresnel treatment a change of variable from the coordinate z , which is the distance on the plate from the geometrical shadow to the fringes, to v is desirable to make a universal plot, the Cornu Spiral, of the relationships involved. The transformation is

$$v = -z/k \quad (7)$$

where

$$k \equiv \sqrt{\frac{\lambda q(p+q)}{2p}} \quad (8)$$

in which λ is the wavelength of light and p and q are the distances defined above. Note that in the schlieren case p is a function of position in the boundary region but q remains constant. Substituting (5) and (6) for p and q , k can be expressed in terms of m , b , λ and f . Then from (1) and (3) it can be put in a more useful form:

$$k = \frac{n-b}{b} \sqrt{\frac{\lambda|f|}{2}} = M \sqrt{\frac{\lambda|f|}{2}} = M \sqrt{\frac{\lambda}{(2a|n''|)}} \quad (9)$$

Absolute value symbols have been used since the same numerical expression is valid for the diverging boundary region yielding source H .

In Fig. 8 the actual phaseplate diaphragm D is considered. The supporting glass plate is not drawn. The source G corresponds to G of Fig. 6 and the point N is the geometrical shadow of the optical edge A of the phaseplate. The Fresnel treatment^{12,13},

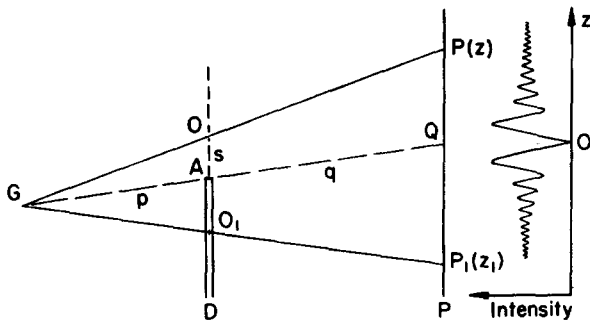


Fig. 8. Fresnel diffraction from a phaseplate.

which is a special case of the more general Kirchhoff treatment, states that the amplitude of the light at a point P on the plate can be obtained by integration of the wave contributions to P from differential elements along the wave front at D originating from G as source. It is assumed that the portions of D that contribute an appreciable amount to the amplitude at P are sufficiently close to the line \overline{GP} that the wave front can be assumed planar. In using the Cornu Spiral, shown schematically for this problem in Fig. 9, the v 's in the third quadrant are negative corresponding to distance s on the wave front below the origin O of the line \overline{GP} . From the geometry in Fig. 8 the relationship between s and z is

$$\frac{s}{z} = \frac{-p}{p+q} \quad (10)$$

so that the conversion of distance on a wave front s to the variable v can be determined, although not needed here, from (7), (8) and (10) as

$$v = \sqrt{\frac{2(p+q)}{pq\lambda}} s \quad (11)$$

The calculation of the amplitude at P_1 will be considered. The distance z_1 is negative,

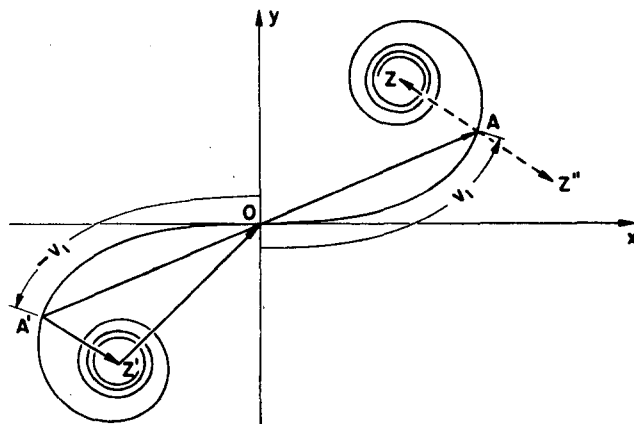


Fig. 9. Cornu Spiral used in solution of the diffraction pattern from a phaseplate.

hence s_1 and v_1 are positive. All the contributions from D to the amplitude at P_1 are (see Fig. 9):

$\overline{Z'O}$: light passing through lower half plane between $-\infty$ and O_1

\overline{OA} : light passing through lower half plane between O_1 and A

\overline{AZ} : light passing through upper half plane between A and $+\infty$
if no phase shift were involved

$\overline{AZ''} = \overline{A'Z'}$: correction of \overline{AZ} for the half wave phase shift present in regions above A compared to regions below A .

$\overline{A'A}$: net amplitude of light at P_1 due to all light passing through phaseplate from $-\infty$ to $+\infty$

This result is generalized for any point P as follows: If $E(v)$ is the amplitude of the vector from the origin of the spiral to the point v , where v corresponds to P , and E_p is the amplitude of the light vector at P then

$$E_p = E(v) - E(-v) = 2E(v) \quad (12)$$

which is the relation given without derivation by WOLTER¹. The location of the maxima and minima of intensity can be found by determining which values of v maximize and minimize $E(v)$. It is usually considered that the 45° line cuts the spiral at the critical values v_c ¹³. For maxima

$$v_{c\max_i} = \sqrt{4i - 5/2} \quad i = 1, 2, 3 \dots \quad (13)$$

For minima

$$v_{c\min_i} = \sqrt{4i - 1/2} \quad i = 1, 2, 3 \dots \quad (14)$$

and on the plate, using (7), (9) and (13) or (14), the location of the i^{th} fringe, counting the geometrical shadow null as zero, is:

$$\begin{aligned} z_{c\text{min}_0} &= 0 \\ z_{c\text{min}_i} &= M \sqrt{\lambda/(2a|n''|)} \sqrt{4i-1/2} & i = 1, 2, 3 \dots \\ z_{c\text{max}_i} &= M \sqrt{\lambda/(2a|n''|)} \sqrt{4i-5/2} & i = 1, 2, 3 \dots \end{aligned}$$

For the opaque upper half plane as schlieren diaphragm the amplitude at P_1 , using again Fig. 9, would be the amplitude of the vector $\overline{Z'O} + \overline{AO} = \overline{Z'A}$. The critical values of v for this vector as the head moves around the spiral are again very close to those cut by the 45° line and hence the spacing of the fringes with a mechanical edge will be the same as with a phaseplate, as observed qualitatively in the experimental section. The relative intensities between the first maximum and first minimum of the phaseplate pattern will be greater than with the knife edge. Thus

$$\text{Knife edge:} \quad \frac{I_{\text{max}_1}}{I_{\text{min}_1}} = \frac{1.34 I_0}{0.78 I_0} = 1.7$$

$$\text{Phaseplate:} \quad \frac{I_{\text{max}_1}}{I_{\text{min}_1}} = \frac{1.73 I_0}{0.59 I_0} = 2.9$$

Thus the phaseplate does not eliminate diffraction effects, in fact intensifying the fringe pattern, but utilizes diffraction to enable a null point registration of true boundary positions.

SUMMARY

An inexpensive practical phaseplate available commercially is described. Illustrations are given of its use in electrophoresis and ultracentrifugation equipments as a schlieren diaphragm—the operational heart of the schlieren optical system. Practically the use of the phaseplate is warranted when a. high magnification angles are used b. the refractive index gradient curve is steep c. disturbances in the cell are to be seen most clearly. Theoretically, the phaseplate confirms concepts as to the nature of the diffraction fringes from any schlieren diaphragm since it operates on diffraction due to defocusing of the light source image by the lens action of the gradient. DISTÈCHE's and WOLTER's theory of the fringes are contrasted. The phaseplate also makes more clear the nature of the anomaly of schlieren patterns near the baseline which show a different shape of curve depending upon the orientation of the opaque edge.

RÉSUMÉ

Une lame à diffraction pratique et bon marché, existant dans le commerce, est décrite. Des exemples de son emploi dans l'électrophorèse et l'ultracentrifugation comme "schlierendiaphragm" — pièce principale d'un système optique schlieren — sont donnés. Du point de vue pratique, l'usage de cette lame peut être recommandé, a. lorsque des angles importants d'agrandissement sont utilisés, b. lorsque la courbe du gradient d'indice de réfraction a une pente élevée, c. lorsque des troubles de fonctionnement dans la cellule doivent être décelés plus clairement. Du point de vue théorique, la lame de diffraction confirme les hypothèses relatives à la nature des franges de diffraction d'un "schlierendiaphragm" quelconque, puisqu'elle agit sur la diffraction due au déplacement de l'image de la source lumineuse par l'action de lentille du gradient. Les théories de DISTÈCHE et de WOLTER sur les franges sont mises en opposition. La lame rend également plus claire la nature de l'anomalie des diagrammes de schlieren au voisinage de l'origine qui donne à la courbe une forme dépendant de l'orientation du bord opaque.

ZUSAMMENFASSUNG

Eine praktische, billige und im Handel erhältliche Phasenplatte wird beschrieben. Es werden Abbildungen von seiner Verwendung als ein Schlierendiaphragma, dem wirkungsvollsten Teil eines optischen Schlierensystems, bei Ausrüstungen für Elektrophorese und Ultrazentrifugation gegeben.

References p. 35.

Die Verwendung der Phasenplatten ist praktisch gerechtfertigt, wenn a. grosse Vergrößerungswinkel benützt werden, b. die Kurve des Brechungsindexgradienten steil ist und c. die Störungen in der Zelle am deutlichsten zu sehen sind. Theoretisch bestätigt die Phasenplatte Begriffe, die die Natur der Streuungsränder der Schlierendiagramme betreffen, da sie auf die Streuung, die dem Unschärfwerden des Lichtquellenbildes zuzuschreiben ist durch die Linsenwirkung des Gradienten wirkt. Die Theorien der Ränder von DISTÈCHE und WOLTER werden einander gegenübergestellt. Die Phasenplatten machen ebenfalls die Art der Anomalie der Schlierenmuster in der Nähe der Grundlinie deutlicher, die eine verschiedene, von der Orientierung des undurchsichtigen Randes abhängige Kurvenform zeigen.

REFERENCES

- ¹ H. WOLTER, *Ann. Physik*, 7 (1950) 182.
- ² L. G. LONGSWORTH, *Ind. Eng. Chem., Anal. Ed.*, 18 (1946) 219.
- ³ O. LAMM, *Z. physik. Chem.*, A, 138 (1928) 313.
- ⁴ H. SVENSSON, *Arkiv Kemi, Mineral. Geol.*, 22A (1948) No. 10.
- ⁵ L. G. LONGSWORTH, *J. Am. Chem. Soc.*, 65 (1943) 1755.
- ⁶ W. KOSSEL AND K. STROHMAIER, *Z. Naturforsch.*, 6A (1951) 504.
- ⁷ O. ARMBRUSTER, W. KOSSEL AND K. STROHMAIER, *Z. Naturforsch.*, 6A (1951) 509.
- ⁸ E. G. PICKELS, W. F. HARRINGTON AND H. K. SCHACHMAN, *Proc. Nat. Acad. Sci.*, 38 (1952) 943.
- ⁹ G. KEGELES AND F. GUTTER, *J. Am. Chem. Soc.*, 73 (1951) 3770.
- ¹⁰ J. W. GOFMAN *et al.*, *Science*, 111 (1950) 166.
- ¹¹ A. DISTÈCHE, *Biochim. Biophys. Acta*, 3 (1949) 146.
- ¹² F. A. JENKINS AND H. E. WHITE, *Fundamentals of Physical Optics*, McGraw-Hill, 1937.
- ¹³ J. VOLASEK, *Introductory Theoretical and Experimental Optics*, John Wiley, 1949, pp. 172-185.

Received December 23rd, 1953